www.vbripress.com/aml, DOI: 10.5185/amlett.2016.6208 Published online by the VBRI Press in 2016

Characterization and synthesis of Bi_2Se_3 topological insulator thin film using thermal evaporation

Bushra Irfan and Ratnamala Chatterjee*

Department of Physics, Indian Institute of Technology Delhi (IITD), New Delhi 110016, India

*Corresponding author. Tel: (+91) 11-2659-1354; Fax: (+91) 11-2659-1114; E-mail: rmala@physics.iitd.ac.in

Received: 19 October 2015, Revised: 06 February 2016 and Accepted: 26 May 2016

ABSTRACT

Topological insulators are the new phase of matter with bulk insulating and conducting surface states. Among the known three dimensional topological insulators, bismuth selenide (Bi_2Se_3) is one of the most promising materials for studying topological insulating properties. Bi_2Se_3 thin films are grown using thermal evaporation technique and atomically smooth films are obtained by post annealing treatment. Pure phase of Bi_2Se_3 is confirmed using x-ray diffraction; Raman spectroscopy shows a strong intensity of A^1_{1g}, E^2_g and A^2_{1g} modes in Bi_2Se_3 thin films. The surface studies on these films are carried out using scanning electron microscopy and atomic force microscopy. X-ray photoelectron spectroscopy (XPS) is used for elemental analyses in Bi_2Se_3 thin film. The surface quality of the film is improved with plasma etching (i.e. argon etching) in XPS. High quality Bi_2Se_3 thin films can be used further for investigation on transport properties of topological insulators. Copyright © 2016 VBRI Press.

Keywords: Thin film; Bi_2Se_3; topological insulators.

Introduction

Bismuth selenide (Bi_2Se_3) is a well known thermoelectric material and recently developed more attention with the discovery of three dimensional topological insulators. Topological insulator (TI) is a new phase of matter characterized by conducting surface states with bulk insulating [**1, 2**]. In TIs the surface states are protected by time reversal symmetry [**3**] and back scattering is prohibited due to strong spin orbit coupling that result in dissipation less transport and hence it has application in thermo-electrical devices, spintronics and quantum computation [**4,5**]. Bi_2Se_3 is confirmed as three dimensional topological insulators both theoretically [**6**] as well as experimentally [**7**]. Various surface sensitive techniques such as angled resolved photoemission spectroscopy (ARPES) [**8, 9**] and scanning tunneling microscopy (STM) [**5, 10**] is used to study the surface properties of topological insulators. Till date, most of the studies on TIs using ARPES measurements are performed on the surface of cleaved single crystals. However, to study the surface states of topological insulators fabricating thin films or nanostructures is another approach and can be used in device application. In thin films large surface to volume ratio suppresses the bulk conduction and enhanced the surface properties. For studying the topological insulating properties in thin films it is necessary to have crystalline thin film i.e. topological insulating properties can be studied only in crystalline thin films. Polycrystalline thin films have application in thermoelectric devices. Molecular beam epitaxial (MBE) is one of the most popular techniques to grow single crystalline thin films by minimizing crystal defects [**11-14**]. Recently a flash-evaporation technique is also used to grow Bi_2Se_3 thin films for studying topological insulating properties [**15**]. Thin films of Bi_2Se_3 grown by MBE technique have shown quantum transport phenomenon and weak antilocalization effect [**16-18**]. The other methods used to synthesize Bi_2Se_3 films such as chemical bath deposition [**19**], electro-deposition [**20**], successive ionic layer adsorption and reaction [**21**], solvo thermalization [**22**] and reactive evaporation [**23**] method generally synthesized a polycrystalline film which is mainly used for thermoelectric applications and does not show any topological insulating properties [**11**]. Therefore, growing high quality single crystalline thin film is necessary for studying the surface properties of topological insulators.

In this work, we report a growth of single crystalline Bi_2Se_3 thin film on Si/SiO_2 substrate using thermal evaporation. We found atomically smooth thin films of Bi_2Se_3 after post annealing treatment, which can be used for studying the topological insulating properties. The advantage of thermal evaporation over MBE is that, it is a simple technique and does not require an ultra high vacuum. Bi_2Se_3 films grown by thermal evaporation technique are characterized using x-ray diffraction (XRD), Raman spectroscopy, scanning electron microscopy (SEM), atomic force microscopy (AFM) and x-ray photon electron spectroscopy (XPS). Such high quality thin film can be further used to study the physical properties of topological insulators, such as two-dimensional transport behaviors.

Experimental

Sample preparation

Bi_2Se_3 single crystals are used as a precursor for thin film growth. High quality single crystals of Bi_2Se_3 are grown using modified Bridgeman technique as described in our previous reports [**24-26**]. Bi_2Se_3 thin film are deposited on Si/SiO_2 substrate at a base pressure ~ 10^{-3} Pa. Bi_2Se_3 single crystals are then evaporated from molybdenum boat for the growth of thin film using thermal evaporation technique. After the deposition the films were post annealed at 300°C using substrate heater attached with the evaporation system.

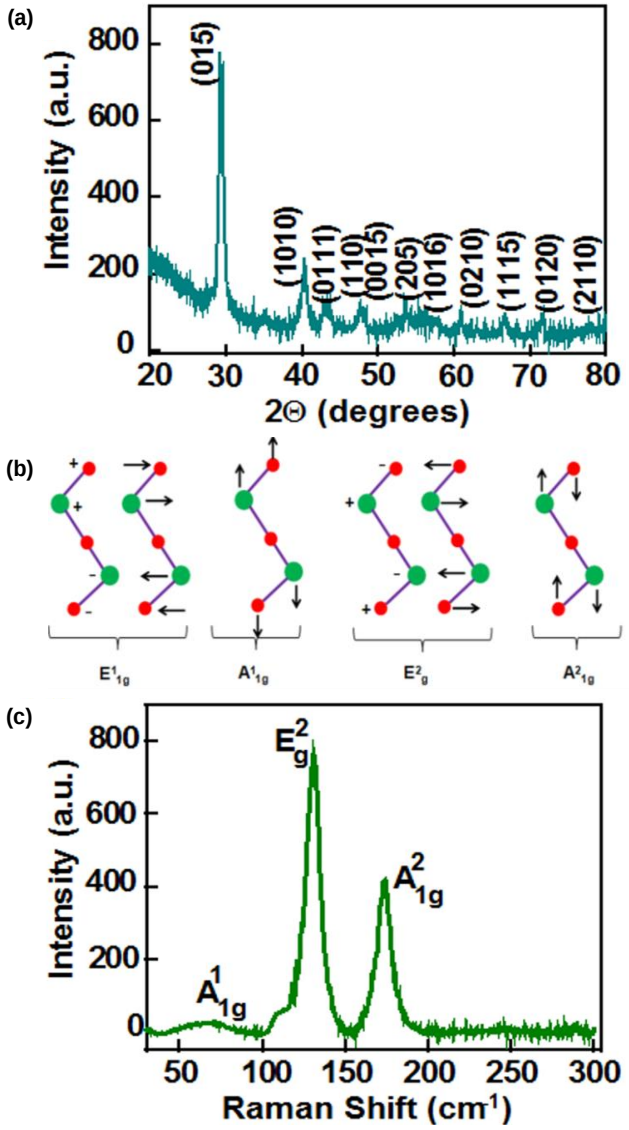

Fig. 1. (a) XRD pattern of Bi_2Se_3 thin film grown by thermal evaporation and annealed at 300°C; (b) Schematic representation of Raman active modes in rhombohedral structure of Bi_2Se_3; (c) Raman spectra of Bi_2Se_3 thin films shows the three Raman active modes.

Characterization: Structural characterization of Bi_2Se_3 thin films grown by thermal evaporation method are performed using XRD with Cu Kα emission (λ= 1.54 A°) and micro-Raman spectroscopy with an excitation source of 532 nm is used to identify the Raman active modes. AFM and field emission scanning electron microscopy is used to examine the surface morphology. XPS is used to probe for surface chemical analysis.

Results and discussion

Thin films of Bi_2Se_3 is synthesized by thermal evaporation and post annealing treatment exhibit a clear mirror like surface with metallic luster. The film is annealed at a temperature of about 300°C for 4 hours. It is reported [**27**] that at high annealing temperature the edge become rough and thick. To investigate the formation of Bi_2Se_3 phase, the films are investigated using x-ray diffraction. A typical XRD pattern of Bi_2Se_3 thin film grown using thermal evaporation can be seen in **Fig. 1(a)**. The sharp peaks indicate a crystalline thin film and all the peaks can be indexed for rhombohedral structure of Bi_2Se_3 with $R\bar{3}m$ space group with lattice parameters a = 4.127 A° and c = 28.58 A°, which agrees well with the reported values (JCPDS 33-0214). There is no impurity peak detected which indicates that Bi_2Se_3 is in pure phase.

Bismuth selenide (Bi_2Se_3) is a layered material that consists of five atoms per unit cell such as Se-Bi-Se-Bi-Se forming quintuple layers and each repeating unit is held together with weak Van der Waals force. Thus, for these types of material one can have 15 zone centre phonon branches in phonon dispersion relation with three acoustic and 12 optical phonons. Group theory predicts that out of these 12 zone center optical phonons, 4 are Raman active and four are infra red (IR) active. The irreducible representation for zone center phonon can be written as [**28**]

$$\Gamma = 2E_g + 2A_{1g} + 2E_u + 2A_{1u} \quad (1)$$

where, "g" is gerade mode and "u" is ungerade mode, gerade modes are Raman active mode and u mode is infra red active modes. From eq. (1) the four Raman active modes in Bi_2Se_3 are 2 A1g + 2 Eg modes. A_{1g} modes represent the atomic vibrations along c-axis perpendicular to the layers, whereas E_g modes are atomic vibration in plane as shown in the schematic **Fig. 1(b)**. **Fig. 1 (c)** shows the Raman active modes in Bi_2Se_3 thin films. There are few studies [**29**], in which all the four Raman actives modes were observed. In **Fig. 1(c)** three distinct peaks can be seen clearly at 72, 131 and 175 cm^{-1} that corresponds to A^1_{1g}, E^2_g and A^2_{1g} respectively. The lowest frequency mode E^1_g was not observed possibly due to high Rayleigh background. The thickness dependent study on Raman spectroscopy suggests that as the thickness is lowered the low frequency mode is suppressed by various other phenomena [**30**]. The low frequency E^1_g mode has very low intensity and is not observed in most of the reports available in literature [**31, 32**]. The high intensity peaks at 72, 131 and 175 cm^{-1} corresponding to A^1_{1g}, E^2_g and A^2_{1g} in Bi_2Se_3 thin films reveal a formation of good quality Bi_2Se_3 thin film.

The SEM image of Bi_2Se_3 thin film exhibits a crack free and continuous area as shown in inset of **Fig. 2(a)**. For elemental analysis, the energy dispersive x-ray spectroscopy (EDX) is performed on Bi_2Se_3 thin film. After procuring EDX spectra from Bi_2Se_3 thin film, the atomic ratio of Bi/Se is found to be ~ 2/3 within the accuracy of measurements. From SEM image the microstructures are

not clearly observable (inset of **[Fig. 2(a)**]). To observe the microstructures, Field emission SEM (FESEM) is used to analyze Bi_2Se_3 thin films. The FESEM image of Bi_2Se_3 thin film is taken at different magnification i.e. at 500 nm and 200 nm as shown in **Fig. 2(b, c)** respectively. It is difficult to distinguish the particle size even at 200 nm in FESEM images, which reveal that the particle size is less than 20 nm. However, from SEM and FESEM studies one cannot conclude about surface structure or roughness of the film. AFM is a convenient technique to study the surface roughness of thin films.

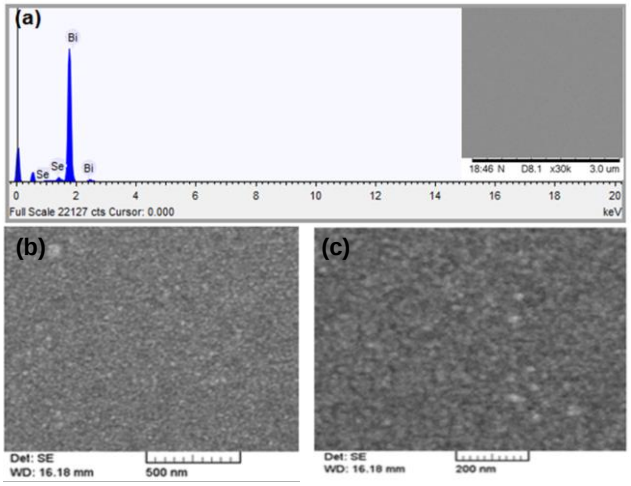

Fig. 2. (a) Elemental dispersive x-ray spectrum of Bi_2Se_3 thin film, an inset shows the SEM image of the film; **(b)** FESEM image at magnification 500 nm; **(c)** FESEM image taken at 200 nm to observe the microstructure.

The surface topography of thin film is examined using atomic force microscopy. AFM image of 2D and 3D plots of Bi_2Se_3 thin film is shown in **Fig. 3(a, b)** respectively. From **Fig. 3(a, b)**, a continuous film is observed with no islanding and surface roughness of the film can be calculated. The root mean square roughness (rms) also known as surface roughness is found to be ~ 0.5 nm, which clearly indicate a good quality thin film.

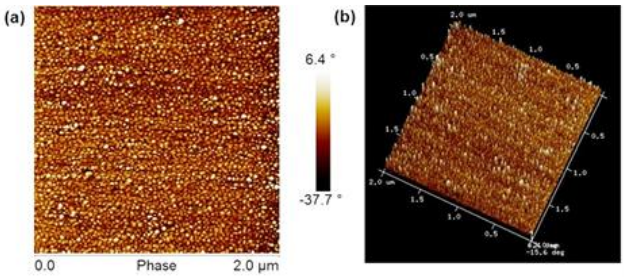

Fig. 3. (a) Two-dimensional AFM image of Bi_2Se_3 thin film; (b) The corresponding 3D AFM image of Bi_2Se_3 thin film.

To understand the chemical stoichiometry of our films, XPS spectrometer (with Mg K_α source) was used and to understand the environmental effect on Bi_2Se_3 thin film XPS spectra was recorded before and after etching with argon plasma. Thin film (thickness ~30 nm) of Bi_2Se_3 is uniformly deposited on Si substrate, so there will be no contribution of the substrate in XPS spectra.

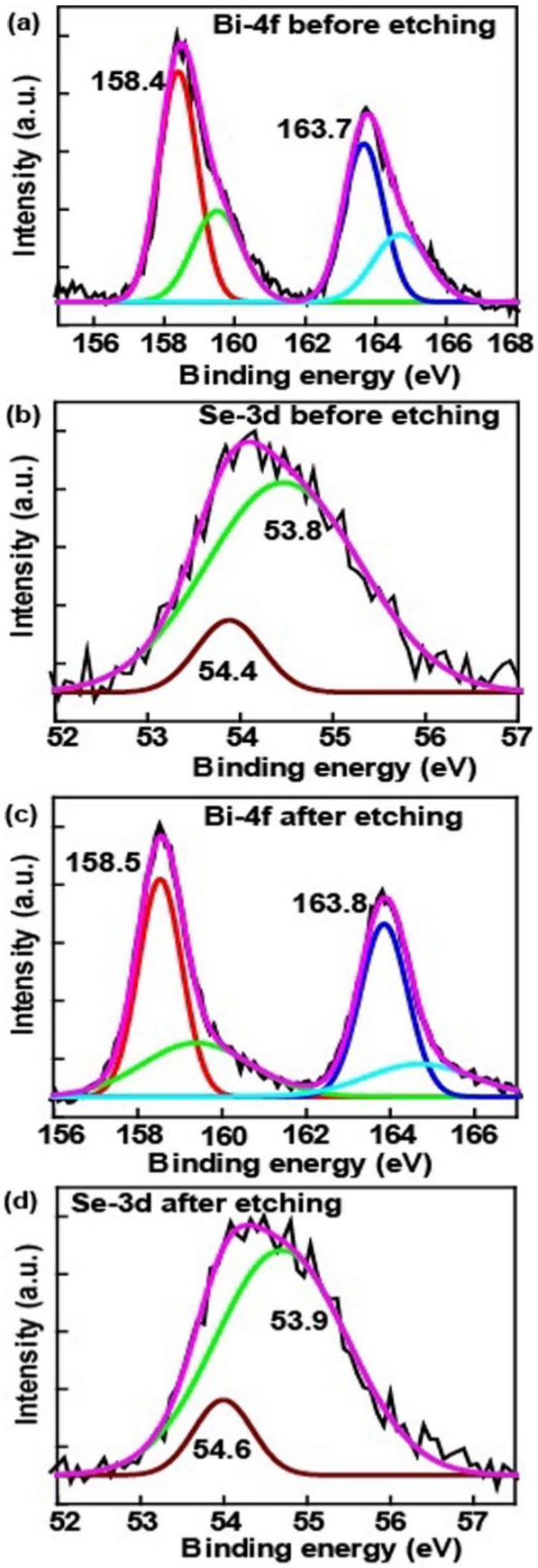

Fig. 4. XPS spectra of Bi_2Se_3 thin film: (a) Bi 4*f* peaks recorded before etching; (b) Se 3*d* peaks recorded before etching; (c) Bi 4*f* peaks taken after etching thin films using argon plasma; (d) Se 3*d* peaks taken after etching Bi_2Se_3 thin film with argon plasma.

Fig. 4(a) shows the XPS spectra of Bi 4*f* core level, which clearly shows two sets of spin-orbit doublet components with peak position at about 158.4 eV and 163.7 eV that corresponds to Bi $4f_{7/2}$ and Bi $4f_{5/2}$ respectively. In addition to the spin orbit doublet a weak intensity peak emerged in the spectrum that overlaps with the major peak of Bi 4*f* photoemission spectra and fitted by Gaussian function. The selenium spectra obtained using XPS is shown in **Fig. 4(b)** and is found to be broad and can be deconvoluated in to two peaks i.e. 53.8eV and 54.4 eV that corresponds to Se $3d_{5/2}$ and Se $3d_{3/2}$ respectively. As Bi_2Se_3 is prone to oxygen, in order to reduce the oxygen, peak the argon ion etching is carried out for 1 min (10 mA, 1kV). The spectrum of etched sample is found to be smoother in comparison to the one without argon plasma etching. The XPS spectra of Bi_2Se_3 shows a similar spin orbit doublet with shift in peak position at 158.5 and 163.8 eV that corresponds to Bi $4f_{7/2}$ and Bi $4f_{5/2}$ respectively. These slight shifts in peak position occur because of surface cleaning by removal of oxygen using argon plasma. The selenium XPS spectrum is also obtained after etching Bi_2Se_3 thin film. A similar broad peak is observed which deconvoluate in to two peaks at 53.8 eV and 54.4 eV that corresponds to Se $3d_{5/2}$ and Se $3d_{3/2}$ respectively as shown in **Fig. 4(c, d)**.

Conclusion

In summary, we have grown a good quality crystalline thin film with thermal evaporation technique using Bi_2Se_3 single crystals as a precursor. This method does not require high a vacuum and a uniform film can be grown with post annealing treatment. Bi_2Se_3 phase is confirmed using x-ray diffraction and Raman spectroscopy shows a strong intensity of A^1_{1g}, E^2_g and A^2_{1g} modes. The surface studies are carried out using SEM and AFM. X-ray photoelectron spectroscopy (XPS) is used for elemental analyses in Bi_2Se_3 thin film. Such high quality single crystalline Bi_2Se_3 thin films are helpful in carrying out further investigation on physical properties, such as weak antilocalization and two-dimensional transport measurements.

Acknowledgements

One of the authors B.I. would like to thank IIT Delhi for providing research fellowship also NRF and XPS facility at IIT Delhi for characterization technique and IUAC Delhi for FESEM measurement.

References

1. Moore, J.E.; *Nature*, **2010**, *464*, 194. **DOI:** 10.1038/nature08916.
2. Fu, L.; Kane, C.; Mele E.; *Phys. Rev. Lett*,. **2007**, *98*, 106803. **DOI:** 10.1103/PhysRevLett.98.106803
3. Qi, X.-L.; Zhang, S.-C.; *Phys. Today*, **2010**, *63*, 33. **DOI:** 10.1063/1.3293411
4. Zhang, N.; Xu, Z.; Feng, Y.; Yao, X. *J. Electroceram*, **2008**, *21*, 609. **DOI:** 10.1007/s10832-007-9249-5
5. Zhang, T.; Cheng, P.; Chen, X.; Jia, J.F.; Ma, X.; He, K.; Wang, L.; Zhang, H.; Dai, X.; Fang, Z.; Xie, X.; Xue, Q.K.; *Phys. Rev. Lett.*, **2009**, *103*, 266803. **DOI:** 10.1103/PhysRevLett.103.266803
6. Zhang, H.; Liu, C.-X.; Qi, X.-L.; Dai, X.; Fang, Z.; Zhang, S.-C.; *Nat. Phys.*, **2009**, *5*, 438. **DOI:** 10.1038/nphys1270
7. Xia, Y.; Qian, D.; Hsieh, D.; Wray, L.; Pal, A.; Lin, H.; Bansil, A.; Grauer, D.; Hor, Y.S.; Cava, R.J.; Hasan, M.Z.; *Nat. Phys.*, **2009**, *5*, 398. **DOI:**10.1038/nphys1274
8. Hsieh, D.; Qian, D.; Wray, L.; Xia, Y.; Hor, Y.S.; Cava, R.J.; Hasan, M.Z.; *Nature*, **2008**, *452*, 970. **DOI:**10.1038/nature06843
9. Chen, Y.L.; Analytis, J.G.; Chu, J.-H.; Liu, Z. K.; Mo, S.-K.; Qi, X.L.; Zhang, H. J.; Lu, D.H.; Dai, X.; Fang, Z.; Zhang, S.C.; Fisher, I.R.; Hussain, Z.; Shen, Z.-X.; *Science*, **2009**, *325*, 178. **DOI:**10.1126/science.1173034
10. Roushan, P.; Seo, J.; Parker, C.V.; Hor, Y.S.; Hsieh, D.; Qian, D.; Richardella, A.; Hasan, M. Z.; Cava, R.J.; Yazdani, A.; *Nature*, **2009**, *460*, 1106. **DOI:**10.1038/nature08308
11. Zhang, G.; Qin, H.; Teng, J.; Guo, J.; Guo, Q.; Dai, X.; Fang, Z.; Wu, K.; *Appl. Phys. Lett.*, **2009**, *95*, 053114. **DOI:** 10.1063/1.3200237
12. Lee, J. J.; Schmitt, F. T.; Moore, R. G.; Vishik, I. M.; Ma, Y.; Shen, Z.X.; *Appl. Phys. Lett.*, **2012**, *101*, 013118. **DOI:** doi/10.1063/1.4733317
13. Kim, Y. S.; Brahlek, M.; Bansal, N.; Edrey, E.; Kapilevich, G.A.; Iida, K.; Tanimura, M.; Horibe, Y.; Cheong, S.W.; Oh, S.; *Phys. Rev. B*, **2011**, *84*, 073109. **DOI:**10.1103/PhysRevB.84.073109
14. Vyshnepolsky, M.; Klein, C.; Klasing, F.; Hanisch-Blicharski, A.; Hoegen, M. H.-V.; *Appl. Phys. Lett.*, **2013**, *103*, 111909 . **DOI:** doi/10.1063/1.4821181
15. Quiqui-B. J.; Lehmann ,T.; Stiller, M.; Spemann, D. Esquinazi, P.; Haussler, P.; *J. Appl. Phys*., **2015**, *117*, 073501. **DOI:**10.1063/1.4908007
16. Liu, M.; Chang, C. Z.; Zhang, Z.; Zhang, Y.; Ruan, W.; He, K.; Wang, L. L.; Chen, X.; Jia, J.F.; Zhang, S.C.; Xue, Q.K.; Ma, X.; Wang, Y.; *Phys. Rev. B*, **2011**, *83*, 165440. **DOI:**10.1103/PhysRevB.83.165440
17. Chen, J.; Qin, H.; Yang, F.; Liu, J.; Guan, T.; Qu, F.; Zhang, G.; Shi, J.; Xie, X.; Yang, C.; Wu, K.; Li, Y.; L. Lu, L.; *Phys. Rev. Lett.* **2010**, *105*, 176602. **DOI:**10.1103/PhysRevLett.105.176602
18. Jerng, S.-K.; Joo, K.; Kim, Y.; Yoon, S.-M.; Lee, J. H.; Kim, M.; J. S. Kim, J.S.; Yoon, E.; S.-H. Chun, S.-H.; Kim, Y. S.; *Nanoscale*, **2013**, *5*, 10618. **DOI:** 10.1039/C3NR03032F
19. Nkum, R. K.; Adimado, A. A.; H. Totoe, H.; *Mater. Sci. Eng. B*, **1998**, *55*, 102. **DOI:** 10.1016/S0921-5107(98)00193-7
20. Killedar,V.V.; Katore, S. N.; Bhosale, C. H.; *Mater. Chem. Phys.*, **2000**, *64*, 166. **DOI:**10.1016/S0254-0584(99)00259-X
21. Sankapal, B.R.; Mane, R.S.; Lokhande, C.D.; *Mater. Chem. Phys.*, **2000**, *63*, 230. **DOI:**10.1016/S0254-0584(99)00226-6
22. Wang, W.; Geng, Y.; Qian, Y.; Xie, Y.; Liu, X.; *Mater. Res. Bull.*, **1999**, *34*, 131-134. **DOI:**10.1016/S0025-5408(98)00203-7
23. Jacob John, K.; Pradeep, B.; Mathai, E.; *Solid State Commun.*, **1993**, *85*, 879-881. **DOI:**10.1016/0038-1098(93)90196-T
24. Irfan, B.; Sahoo, S.; Gaur, A. P. S.; Ahmadi, M.; Guinel, M. J.-F.; Katiyar, R.S.; Chatterjee, R.; *J. Appl. Phys.*, **2014**, *115*, 173506. **DOI:**10.1063/1.4871860
25. Irfan, B.; Joshi, B.P.; Thamizhavel, A.; Deshmukh, M.; Chatterjee, R.; *Solid State Commun*., **2015**, *220*, 45-48. **DOI:**10.1016/j.ssc.2015.07.007
26. Irfan, B.; Chatterjee, R.; *Appl. Phys. Lett.*, **2015,** *107*, 173108. **DOI:**10.1063/1.4934569
27. Zhang, M.; Lv, L.; Wei, Z.; Guo, C.; Yang, X.; Zhao, Y.; *Mater. Lett.*, **2014**, *123*, 87-89. **DOI:**10.1016/j.matlet.2014.02.108
28. Köhler, H.; Becker, C. R.; *Phys. Status Solidi B*, **1974**, *61*, 533-537. **DOI:**10.1002/pssb.2220610218
29. Zhang, J.; Peng, Z.; Soni, A.; Zhao, Y.; Xiong, Y.; Peng, B.; Wang, J.; Dresselhaus, M. S.; Xiong, Q.; *Nano Lett.*, **2011**, *11*, 2407-2414. **DOI:**10.1021/nl200773n
30. Wang, C.; Zhu, X.; Nilsson, L.; Wen, J.; Wang, G.; Shan, X.; Zhang, Q.; Zhang, S.; Jia, J.; Xue, Q.; *Nano Res*,. **2013**, *6*, 688-692. **DOI:**10.1007/s12274-013-0344-4
31. Vilaplana, R.; Santamaría-Pérez, D.; Gomis, O.; Manjón, F.J.; González, J.; Segura, A.; Muñoz, A.; Rodríguez-Hernández, P.; Pérez-González, E.; Marín-Borrás, V.; Muñoz-Sanjose, V.; Drasar, C.; Kucek, V.; *Phys. Rev. B*, **2011**, *84*, 184110.

DOI:10.1103/PhysRevB.84.184110
32. Kim, Y.; Chen, X.; Wang, Z.; Shi, J.; Miotkowski, I.; Chen, Y.P.; Sharma, A.; Lima Sharma, A.L.; Hekmaty, M.A.; Jiang, Z.; Smirnov, D.; *Appl. Phys. Lett.*, **2012**, *100*, 071907.
DOI:10.1063/1.3685465